

## Investigating Microfluidic Supercritical Antisolvent process: *in situ* micro-experiments and High Performance computing

**A. Erriguible<sup>a,b</sup>, T. Jaouhari<sup>b</sup>, S. Glockner<sup>a</sup>, S. Fery-Forgues<sup>c</sup>, C. Aymonier<sup>b</sup>, S. Marre<sup>b</sup>**

*a. CNRS, Univ. Bordeaux, Bordeaux INP, I2M, UMR 5295, F-33600, Pessac Cedex, France*

*b. CNRS, Univ. Bordeaux, Bordeaux INP, ICMCB, UMR 5026, F-33600, Pessac Cedex, France*

*c. SPCMB, UMR CNRS 5068, Université Toulouse III Paul-Sabatier, 118, route de Narbonne, 31062 Toulouse Cedex 09, France*

### 1. Introduction

Although supercritical anti-solvent (SAS) processes are mainly used in semi-continuous mode in macroscopic reactors, continuous micro- and microscale reactors are now emerging as one of the most promising ways to intensify and better control the process. As these microfluidic systems reduce time and space scales, their effectiveness in controlling mixing and improving process performance is obvious. This is particularly true for materials synthesis, where rapid and homogeneous mixing is the key to achieving a narrow particle size distribution. A recent study<sup>1</sup> showed that a combination of both types of intensification, supercritical fluids and microfluidic reactors ( $\mu$ SAS), can significantly improve the performance and reproducibility of antisolvent processes. Furthermore, it has recently been shown that turbulent conditions can be achieved in high-pressure microfluidic devices<sup>2</sup>, allowing for ultra-fast mixing times of the order of  $10^{-4}$ - $10^{-5}$  s, which are very favourable for the synthesis of organic nanoparticles. In this system, the nucleation and growth mechanisms are responsible for the size and morphology of the nanoparticles, which directly affect the solubility and bioavailability of organic compounds. Therefore, the study of these mechanisms is essential to better understand the impact of operating parameters on the final size of the synthesised particles. For this, a coupled experimental/simulation approach is used. The high-pressure microfluidic platform provides optical access and well-controlled operating conditions to study precipitation *in situ*. Our experimental strategy is to combine microfluidics with an organic fluorogen to visualise *in situ* precipitation of organic fluorescent nanoparticles (FONs) in the reactor. To do this, we take advantage of the specific optical properties of dye molecules that exhibit aggregation-induced emission (AIE) effects, i.e. molecules that emit much more strongly in the aggregated and solid state than in solution. The experimentally obtained fluorescence intensity fields are then compared to a direct numerical simulation, capturing all mixing scales and considering all implicit phenomena, i.e. thermo-hydrodynamics as well as nucleation and growth. This comparison leads to a better understanding and identification of the nucleation mechanisms involved in the  $\mu$ SAS process<sup>3</sup>.

### 2. Materials and Methods

A Pyrex/silicon microchip was manufactured following standard photolithography / wet etching / anodic bonding protocol<sup>4</sup>. The microreactor is used as a micromixer to contact the concentrated solution (Tetrahydrofuran + FONs) and the antisolvent sc-CO<sub>2</sub>, benefiting from ultra-low mixing times at supercritical conditions. The design of the reactor (Fig. 1a) includes a main channel (trapezoidal crossed section, 200  $\mu$ m deep, 350  $\mu$ m wide at the top of the channel) in which a silica capillary (ID: 100  $\mu$ m, OD: 170  $\mu$ m) is inserted. The microreactor is placed under a confocal microscope (Fig 1.b) for the *in situ* imaging of the FONs fluorescence during the precipitation process. A motorized Leica SP8 confocal microscope is used for direct visualization using an excitation laser diode emitting at 405 nm with an 10x objective, leading to a resolution of  $\approx 1$  pixel/ $\mu$ m. We performed temporal analysis of the fluorescence intensities to quantify a concentration field of fluorescent particles. This very important result is compared with the particle field calculated by the simulation and makes it possible to localize the nucleation/precipitation zones in the reactor. This analysis element is essential in the validation of the precipitation models used. The numerical approach allows taking into account all the physical phenomena involved in the process. The method consists in the coupling between a computational fluid dynamics (CFD) code, to consider the thermo-hydrodynamic effects, and a population balance equation (PBE) to take into account the nucleation and growth of particles. A High Performance computing homemade code (Notus) is used to capture all the mixing scales up to the Batchelor one<sup>5</sup>.

### 3. Results and discussion

First, precipitation of the FONs, is performed at 40°C, 100 bar. The recovered powders were characterized by transmission electron microscopy. We obtained a mean size of 16 ( $\pm$  4) nm. The *in situ* experiment concerned the determination of the fluorescence intensity fields in the microchannel. Fig. 1.c displays the intensity mapping obtained experimentally by averaging instantaneous fields. These data allow us to locate the areas where the solid fluorescent particles are present. The intensity field increases with the particle concentration. In fig. 1, the abscissa 0 corresponds to the outlet of the injection capillary. The first result obtained shows a very strong intensity signal at the injector outlet. This means that compound BZX precipitates out of the injector. It is important to note that the fluorescence intensity drops rapidly as soon as it leaves the injector, at a distance of about 200-300  $\mu$ m. In Fig.1.d, we have represented the particle concentration in the channel obtained by numerical simulation. The comparison of the numerical and experimental fields shows a great coherence in terms of location of the nucleation/precipitation zones. We observe a very strong mixing of the FONs as soon as the compound leaves the injection on an extremely short length scale, thus with a very short time. The particles are then generated in this zone, which corresponds to a zone of important supersaturation. Simulation and reveals very short micromixing times, lower than  $10^{-4}$  s, and shows us that the intense mixing is located at the periphery of the central jet. These remarkable zones are well reflected in both numerical and experimental mappings. The mixing conditions are here very good, fast and total, and show the importance of hydrodynamics in this type of reactor.

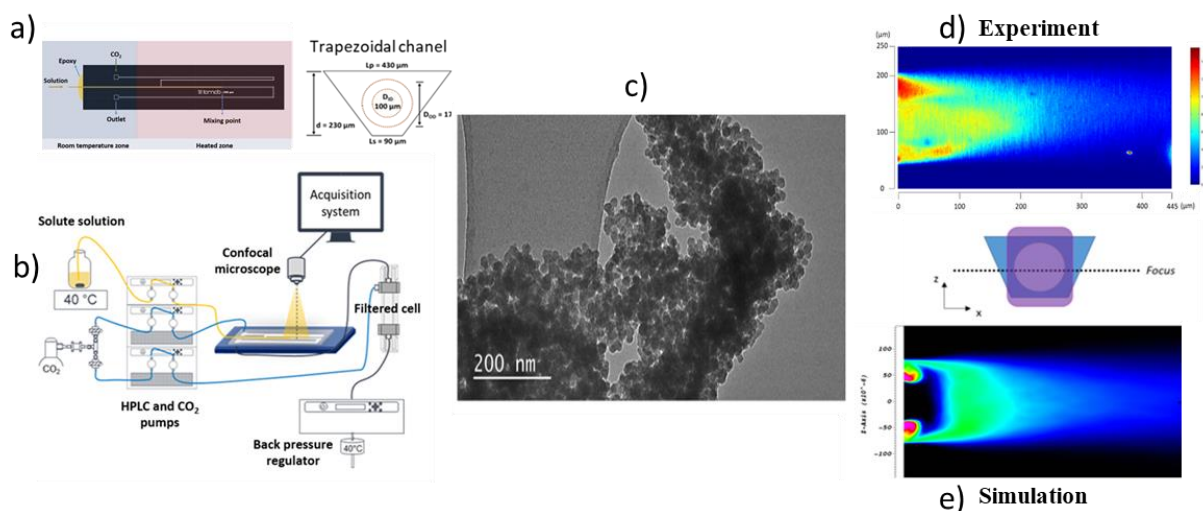


**Figure 1.** a) High pressure microchip; b) Schema of  $\mu$ SAS set-up with confocal microscope for direct visualization; c) TEM images of recovered powders; d) Experimental mapping of time averaged intensity field of particles in the microchannel; e) Simulation of particle number field in the microchannel

### 4. Conclusions

The  $\mu$ SAS process has shown its ability to produce small particles. Moreover, thanks to the optical properties of the chosen fluorescent molecule, we have adopted an *in situ* analysis of the precipitation to have a better understanding of the nucleation and growth phenomena. This experimental result was successfully compared to the prediction given by numerical calculations and showed that the mixing is very fast (less than  $10^{-4}$  s) and takes place totally in a very limited area at the outlet of the injector, leading to a domination of the homogeneous nucleation and thus to the formation of small particles.

### References

1. T. Jaouhari, F. Zhang, T. Tassaing, S. Fery-Forgues, C. Aymonier, S. Marre, A. Erriguible, *Chem. Eng. Journal* **2020**, 397.
2. F. Zhang, S. Marre, A. Erriguible, *Chem. Eng. Journal* **2020**, 382.
3. T. Jaouhari, T. Tassaing, S. Fery-Forgues, C. Aymonier, S. Marre, A. Erriguible, *Chem. Eng. Science* **2022**, 248, art. no. 117240.
4. S. Marre, A. Adamo, S. Basak, C. Aymonier, K.F. Jensen, *Ind. Eng. Chem. Res.* **2010**49, 11310–11320.
5. S. Glockner, A.M.D Jost., A. Erriguible, *Chem. Eng. Journal* **2022**, 431.